



HAL
open science

A study on the low-altitude clouds over the Southern Ocean using the DARDAR-MASK

Yi Huang, Steven T. Siems, Michael J. Manton, Alain Protat, Julien Delanoë

► **To cite this version:**

Yi Huang, Steven T. Siems, Michael J. Manton, Alain Protat, Julien Delanoë. A study on the low-altitude clouds over the Southern Ocean using the DARDAR-MASK. *Journal of Geophysical Research: Atmospheres*, 2012, 117 (D18), pp.D18204. 10.1029/2012JD017800 . hal-00724011

HAL Id: hal-00724011

<https://hal.science/hal-00724011>

Submitted on 26 Aug 2020

HAL is a multi-disciplinary open access archive for the deposit and dissemination of scientific research documents, whether they are published or not. The documents may come from teaching and research institutions in France or abroad, or from public or private research centers.

L'archive ouverte pluridisciplinaire **HAL**, est destinée au dépôt et à la diffusion de documents scientifiques de niveau recherche, publiés ou non, émanant des établissements d'enseignement et de recherche français ou étrangers, des laboratoires publics ou privés.

A study on the low-altitude clouds over the Southern Ocean using the DARDAR-MASK

Yi Huang,¹ Steven T. Siems,¹ Michael J. Manton,¹ Alain Protat,² and Julien Delanoë³

Received 18 March 2012; revised 6 July 2012; accepted 10 August 2012; published 21 September 2012.

[1] A climatology of the thermodynamic phase of the clouds over the Southern Ocean (40–65°S, 100–160°E) has been constructed with the A-Train merged data product DARDAR-MASK for the four-year period 2006–2009 during Austral winter and summer. Low-elevation clouds with little seasonal cycle dominate this climatology, with the cloud tops commonly found at heights less than 1 km. Such clouds are problematic for the DARDAR-MASK in that the Cloud Profiling Radar (CPR) of CloudSat is unable to distinguish returns from the lowest four bins (heights up to 720–960 m), and the CALIOP lidar of CALIPSO may suffer from heavy extinction. The CPR is further limited for all of the low-altitude clouds (tops below 3 km) as they are predominantly in the temperature range from 0°C to –20°C, where understanding the CPR reflectivity becomes difficult due to the unknown thermodynamic phase. These shortcomings are seen to flow through to the merged CloudSat-CALIPSO product. A cloud top phase climatology comparison has been made between CALIPSO, the DARDAR-MASK and MODIS. All three products highlight the extensive presence of supercooled liquid water over the Southern Ocean, particularly during summer. The DARDAR-MASK recorded substantially more ice at cloud tops as well as mixed-phase in the low-elevation cloud tops in comparison to CALIPSO and MODIS. Below the cloud top through the body of the cloud, the DARDAR-MASK finds ice to be dominant at heights greater than 1 km, especially once the lidar signal is attenuated. The limitations demonstrated in this study highlight the continuing challenge that remains in better defining the energy and water budget over the Southern Ocean.

Citation: Huang, Y., S. T. Siems, M. J. Manton, A. Protat, and J. Delanoë (2012), A study on the low-altitude clouds over the Southern Ocean using the DARDAR-MASK, *J. Geophys. Res.*, 117, D18204, doi:10.1029/2012JD017800.

1. Introduction

[2] The low-altitude clouds over the Southern Ocean (tops below 3 km) offer a significant contrast in the albedo to the underlying ocean surface. These clouds are not only a primary component of the energy and water budgets over the Southern Ocean (SO), but also help define the meridional fluxes of energy and water to the Antarctic. Yet as detailed in *Trenberth and Fasullo* [2010], the clouds over the SO are poorly represented in both present-day reanalyses and coupled global climate models; the climate models and reanalyses simulate a fractional cloud coverage of approximately 80% while the observations produce a result of

approximately 90%. This bias in cloud cover is, in turn, directly responsible for an overestimate in the present-day simulation of the absorbed shortwave radiation over the SO. The poor representation of the energy and water budget over the SO, a region covering 15% of the Earth's surface, creates uncertainties in climate and weather simulations of the Antarctic [*Tietäväinen and Vihma*, 2008].

[3] *Mace* [2010] studied the radiative and microphysical properties of these clouds over the SO employing an integration of active remote observations from CloudSat [*Im et al.*, 2006], Cloud-Aerosol Lidar and Infrared Pathfinder Satellite Observations (CALIPSO) [*Winker et al.*, 2007] and passive remote observations from the Advanced Microwave Scanning Radiometer (AMSR-E) [*Wentz and Meissner*, 2000], the Moderate Resolution Imaging Spectroradiometer (MODIS) [*Platnick et al.*, 2003] and the Clouds and the Earth's Radiant Energy System (CERES) [*Wielicki et al.*, 1998]. When comparing a 20° × 20° region of the SO with that over the North Atlantic, *Mace* [2010] concluded that there was a 'high degree of similarity in cloud occurrence statistics, in cloud properties, and in the radiative effects of the clouds.' This conclusion is perhaps remarkable when reflecting upon the inherent differences between the North Atlantic and the SO. The atmosphere over the SO is not only essentially free of anthropogenic

¹Monash Weather and Climate, Monash University, Monash, Victoria, Australia.

²Centre for Australian Weather and Climate Research, Melbourne, Victoria, Australia.

³Laboratoire Atmosphere, Milieux, et Observations Spatiales, IPSL/UVSQ/CNRS, Guyancourt, France.

Corresponding author: Y. Huang, Monash Weather and Climate, Monash University, Monash, Vic 3800, Australia. (vivian.huang@monash.edu)

aerosol emissions, but even terrestrial aerosol emissions such as dust. Field observations of the Cloud Condensation Nuclei (CCN) over the SO [e.g., *Yum and Hudson*, 2005; *Gras*, 1995] reveal a highly pristine environment, particularly during the winter season, when there are an order of magnitude fewer CCN than during summer. Unlike the North Atlantic, the cloud microphysics over the SO has been observed to undergo a strong seasonal cycle. The CLAW (Charlson, Lovelock, Andreae and Warren) [*Charlson et al.*, 1987; *Ayers and Cainey*, 2007; *Vallina and Simo*, 2007] hypothesis details the role of the production of dimethylsulfide by phytoplankton during the active summer season, and its impact on the effective radius of the clouds [*Boers et al.*, 1998]. They found that the droplet concentration of suspended cloud droplets in summer is three times that of winter, while the effective radius in winter is about 42% larger than that measured in summer.

[4] More recently *Huang et al.* [2012] highlighted that the retrievals of the Cloud Profiling Radar (CPR) of CloudSat are physically limited in observing the low-elevation clouds over the SO. First they illustrated that the CPR commonly dismissed any clouds within the lowest kilometer over the surface that were observed by Cloud-Aerosol Lidar with Orthogonal Polarization (CALIOP) on CALIPSO because the CPR is not able to distinguish the source of reflectivity emanating from near the surface. Next they found that the 500 m vertical resolution of the CPR (oversampled into 240 m bins) [*Stephens et al.*, 2002] was relatively coarse for these clouds, and produced a largely, invariant liquid phase cloud top climatology across the boundary layer of the entire SO. Similarly, the study by *Chan and Comiso* [2011] noted that certain types of low-level clouds that were apparent to MODIS data could not be detected by either CloudSat or CALIPSO, possibly due to the coarse vertical resolution and the low-level ground clutter contamination for the CPR, and the limited sensitivity of CALIOP to the clouds' geometrically thin nature and surface proximity. In particular, these clouds are found over the Arctic region and have optical thicknesses of less than 14, top height altitudes of below 2.5 km, and layer thickness of less than 1 km.

[5] Finally *Huang et al.* [2012] highlighted that virtually all of these low-altitude clouds over the SO exist in the temperature range of 0°C to −20°C. This is particularly problematic for the CPR as it has no direct means of distinguishing between ice and supercooled liquid water (SLW). The classification of the thermodynamic phase requires the use of a temperature-dependent algorithm. Without in situ field observations to validate such algorithms uncertainty will remain, particularly over the highly pristine environment of the SO. For example *Morrison et al.* [2011] (hereinafter MSM11) employed MODIS to build a climatology of the cloud top thermodynamic phase over the SO and found almost no sign of clear glaciation in these low-altitude clouds, not even at high latitudes during the winter. This in itself is of interest, given that the clouds composed of supercooled liquid water over the SO are known to be sensitive to the Hallett-Mossop process of ice multiplication [*Mossop et al.*, 1970]. Similarly *Hu et al.* [2010] identified the near constant presence of SLW over the SO using CALIOP observations.

[6] Motivated by these findings and the continued ambiguity in the observations of clouds from remote sensing instruments on an individual basis, the primary purpose of

this paper is to construct a climatology of both the cloud thermodynamic phase and clouds structure over the SO through the application of the merged A-Train product—raDAR/liDAR-MASK (hereafter DARDAR-MASK) [*Delanoë and Hogan*, 2010]. As a comparison to MSM11, the cloud top thermodynamic phase (CTP) properties are first examined. Below the cloud top, the active sensing capabilities captured in the DARDAR-MASK are employed to explore the structure and thermodynamic phase properties through the depths of the clouds.

[7] The remainder of this paper is organized as follows: Section 2 provides an overview of the merged DARDAR-MASK product, the merging process and retrieval algorithm. Section 3 presents the climatology of CTP over the SO as functions of cloud top height and cloud top temperature (CTT), in comparison to that derived by MODIS in MSM11. Also, statistics of the CTP populations viewed by CALIPSO and its sensitivity to the presence of overhead cirrus is discussed. Section 4 examines the class occurrences and vertical distributions of the thermodynamic phase through the depths of the clouds. Section 5 offers an overall discussion and summary of the key findings.

2. Data

[8] Similar to the merged CloudSat-CALIPSO employed in *Mace* [2010], the DARDAR-MASK data set employs a combination of the CloudSat, CALIPSO and MODIS [*Delanoë and Hogan*, 2010] products to retrieve cloud phase properties. Their algorithm, first proposed in 2008 [*Delanoë and Hogan*, 2008], was originally designed to identify ice clouds on the basis of the synergy of surface-based radar, lidar and infrared radiometer observations. The purpose of adapting the improved technique to A-Train is to examine the state of cloud microphysics from the spaceborne perspective. The DARDAR-MASK returns a range of categories: clear, ground, stratospheric features, insects, aerosols, rain, supercooled liquid water, liquid warm, mixed-phase and ice. The algorithm also permits an uncertain classification, commonly in regions where the radar and lidar signal have been heavily attenuated or are missing.

[9] Data sets employed for merging includes the 94 GHz radar reflectivity from the CloudSat “2B-GEOPROF” product (i.e., the CPR), lidar backscatter coefficient at 532 nm from the CALIPSO Lidar level 1 profile [*Anselmo et al.*, 2006], CALIPSO Lidar level 2 VFM profile (after V3.1.1, “VFM” for “vertical feature mask” [*Hu et al.*, 2009]), the “MODIS-AUX” product (“AUX” for auxiliary of CloudSat archive), with three infrared channels 8.55 μm , 11 μm , 12 μm from MODIS, as well as the “ECMWF-AUX,” also a subset of CloudSat, providing the European Centre for Medium-Range Weather Forecasts (ECMWF) thermodynamic variables. Being a critical input of the DARDAR-MASK classification scheme, it is important to appreciate the potential error in the ECMWF temperature over the SO with limited observations. By employing over 16 years of high-resolution upper air soundings from Macquarie Island (54°62S, 158°85E), *Hande et al.* [2012] suggest that the climatological mean and variability of the ECMWF temperature is generally consistent with the results derived from Macquarie Island soundings, despite a complicated, multilayer structure commonly being underrepresented through the boundary layer. In the merged DARDAR-

MASK algorithm, however, the ECMWF temperature is only used as a diagnosis of cold/warm area (for instance, if the temperature is -5°C we could consider that we are in the cold region), the bias, if there is any, in the partition of MIXED/ICE/SLW (which only occur in cold temperature range) is not critical.

[10] Further, as CloudSat and CALIPSO products are not on exactly the same vertical and horizontal grids, assumptions have been made to align the radar and lidar footprints. If the separation distance between each footprint is greater than 1 km, the collocated profile will not be used. Lidar measurements are averaged horizontally in the CloudSat footprint (typically 3 lidar returned signals are averaged); ECMWF variables are interpolated to the radar resolutions. The vertical resolution is finally re-gridded to 60 m from -1.02 to 25.08 km.

[11] Two examples of CPR reflectivity, CALIOP classification, DARDAR-MASK simplified categorization and along-track MODIS imagery are presented to illustrate the challenges in understanding the ubiquitous low-altitude clouds over the SO. The first example (Figure 1) is taken from a portion of a granule ranging from 65 to 40°S with the longitude ranging from 119.70 to 106.88°E , which is to the south of Australia, during winter (25 August 2008). At both the high latitudes (58 – 62°S) and the low latitudes (42 – 44°S), portions of frontal passages have been intercepted with cloud tops reaching up to 6 km or higher. In between these two regions the lidar detects a near-continuous cloud field with the top ranging between 500 and 2000 m. The lidar also picks up some thick cirrus clouds from 47 to 54°S , which are not picked up by the CPR.

[12] The low-elevation clouds in this middle section from 58 to 44°S illustrate the physical challenges to the CPR identified in Huang *et al.* [2012]. When the cloud top height drops below ~ 960 m, the CPR cannot pick up a valid reflectivity from the dominant radar return. The CPR simply misses the low-altitude clouds between 56 and 58°S and suggests a highly intermittent cloud field from 44 to 50°S . According to the CPR the low-altitude clouds in this range appear to be of roughly uniform thickness due primarily to the coarse 500 m resolution of the CPR. Finally, virtually the entire low-altitude cloud mass lies in the temperature range of 0°C to -20°C , where the cloud could exist as liquid (LIQUID), ice (ICE) or mixed-phase (MIXED). The lidar, on the other hand, suggests a near continuous cloud field with the cloud top being predominantly composed of LIQUID (note: the lidar is unable to distinguish mixed-phase). For this middle section (58 to 44°S), ICE is evident only intermittently from 49 to 53°S , where the cloud top is over 1500 m and the overlying cirrus is thickest. It is unclear to what extent the overlying cirrus is interfering with the sensing of the low-altitude clouds. Given that multilayer cloud coverage is a common feature over the SO [Mace, 2010], this potential bias should be considered.

[13] In this middle range the DARDAR-MASK returns a continuous cloud field ranging from 500 m to 2000 m composed predominantly of mixed-phase along the top where the CPR is able to provide a return (e.g., 51 to 56°S). When the CPR drops out, however, the DARDAR-MASK returns back to supercooled liquid water (SLW) (56 to 58°S) or even

liquid warm (LW) ($\sim 47^{\circ}\text{S}$) when the ECMWF temperature is above 0°C . Through much of this middle range the DARDAR-MASK returns an uncertain (UN) classification beneath cloud top when the CPR is unable to make observations near the surface and the lidar signal is attenuated. In the frontal region at the south of the granule the DARDAR-MASK returns primarily clear glaciation. In the frontal region at the north of the granule the DARDAR-MASK returns mainly mixed-phase and occasionally SLW at cloud top, then glaciation through the clouds and then UN once the CPR and CALIOP fail to give a return. It is interesting to note that in situ observations of clouds composed largely of SLW exist at heights as high as 3 and 4 km in the region of Tasmania [Morrison *et al.*, 2009; Ryan and King, 1997; Mossop *et al.*, 1970].

[14] The second example (Figure 2) is taken on 8 Nov 2008 and runs from 65 to 40°S at a longitude of roughly 149.13 to 136.29°E . This case more vividly illustrates the problem that the CPR has in detecting the low-altitude clouds over the SO. From 40 to 50°S , the lidar detects intermittent cloud cover with cloud bases approximately touching the surface that is almost always missed by the CPR. This cloud deck is above the 0°C level and free from overhead interference. The along-track MODIS image portrays widespread low-level cumulus and stratocumulus. Over the region of 57 to 63°S , both the CPR and CALIOP observe a frontal cloud field with cloud top reaching to 4 km. The lidar finds the top to consist strictly of a layer of SLW whereas the CPR is unable to clearly define the phase given the temperature is between -10 and -15°C . From 59 to 61°S , the cloud field is thick enough that even the CPR becomes attenuated. At the northern and southern edges of this frontal cloud mass, CALIOP and the CPR observe scattered glaciated clouds above 4 km.

[15] Turning to the DARDAR-MASK, a low-level cloud field of intermittent LW, rain (RAIN) and occasionally SLW is observed from 40 to 53°S , consistent with the CALIOP retrievals. In the frontal region (57 to 63°S), the DARDAR-MASK returns a MIXED cloud top with intermittent SLW above a glaciated layer. In the near-frontal clouds (from 64 to 62°S and near 56.5°S), however, when the cloud height drops to ~ 2 km and the temperature rises to above -10°C , the DARDAR-MASK regresses back to SLW at cloud top. UN is assigned at depths where the signal from CALIOP is thoroughly attenuated and the CPR is attenuated or affected by clutter contamination (e.g., 59 to 61°S).

[16] Despite the potential biases introduced by multilayer situations that may cause lidar attenuation or even extinction and low-level ground clutter contamination for the radar, the statistical importance of these conditions is still unknown and has to be thoroughly assessed. Given the fact that a ground-based station that can readily be deployed for verification is not available in this remote area, it is important to develop a better understanding through an inter-comparison of different spaceborne sensors. An attempt of this paper, therefore, is to construct a climatological comparison between the merged A-train and MODIS only (MSM11) observations, to appreciate the statistical importance of these biases. While a direct comparison between different instruments might have its own limitations (considering the differences in footprints,

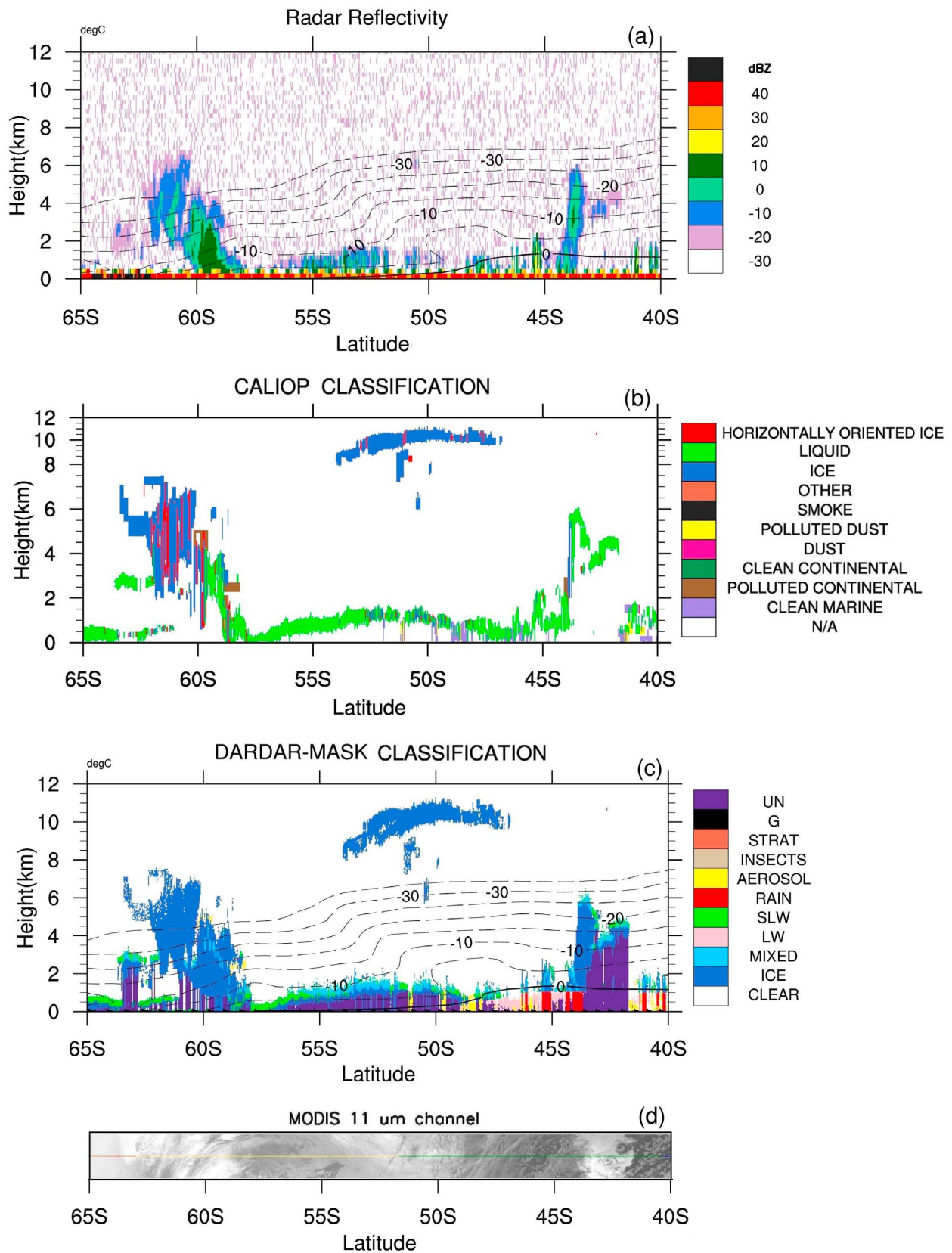


Figure 1. An example of the DARDAR-MASK simplified categorization, CloudSat CPR reflectivity, CALIOP classification and along-track MODIS visible image of a portion of a A-Train granule over the Southern Ocean on 25 August 2008. (a) CloudSat CPR reflectivity. (b) CALIOP classification. (c) DARDAR-MASK simplified categorization. (d) Along-track MODIS 11 μm imagery.

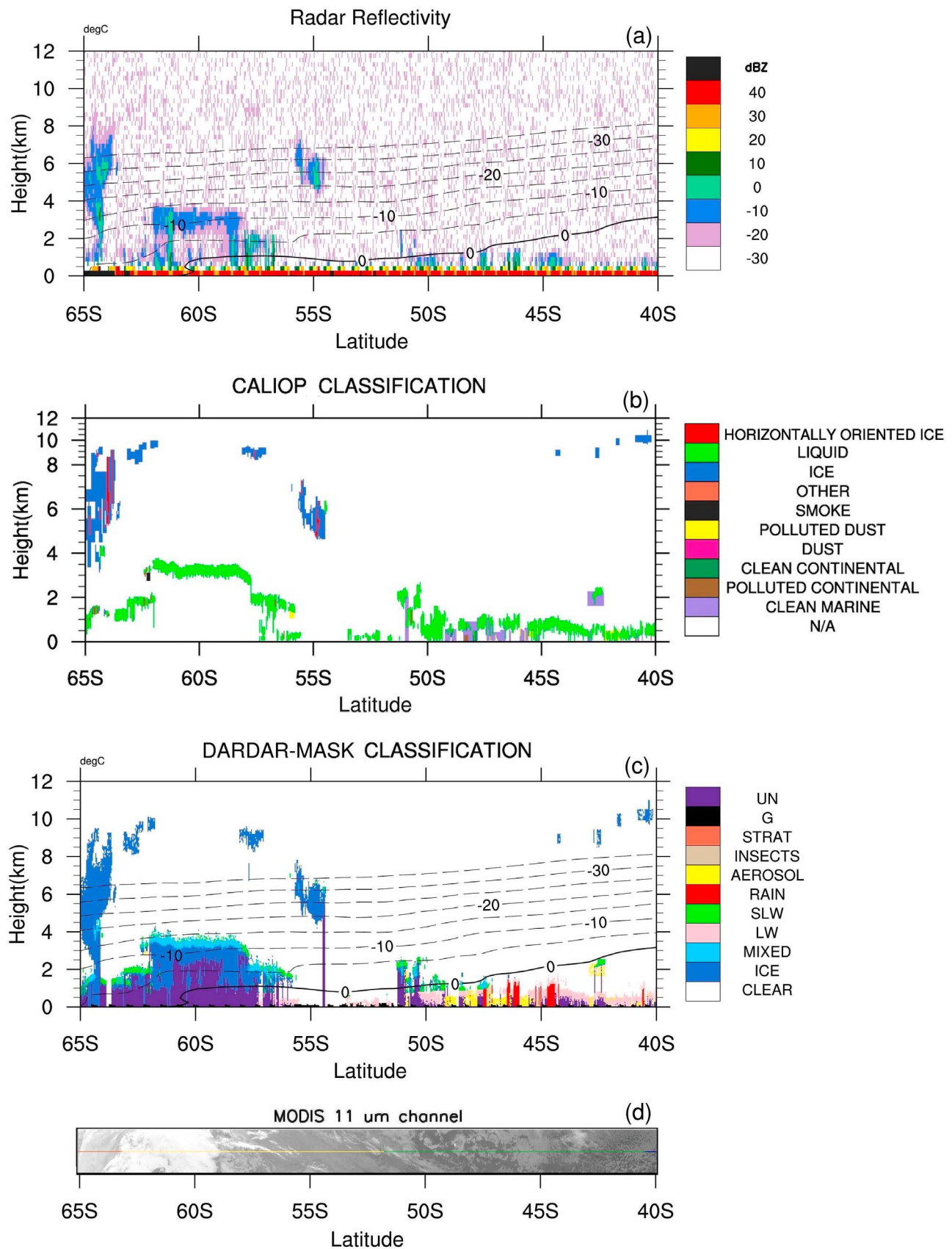


Figure 2. Same as Figure 1 for a portion of a A-Train granule over the Southern Ocean on 08 Nov 2008.

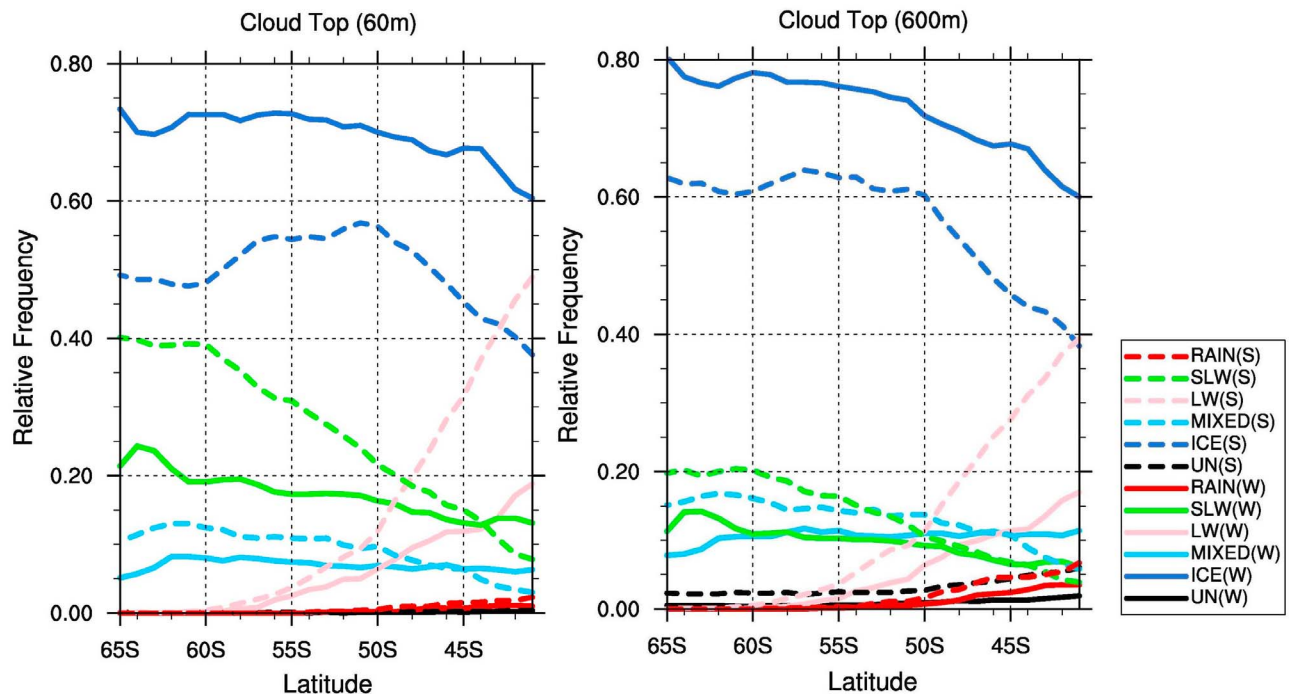


Figure 3. Relative Frequencies (RFs) of the cloud top thermodynamic phase classes of ice (ICE), mixed-phase (MIXED), liquid warm (LW), supercooled liquid water (SLW), rain (RAIN) and uncertainty (UN) categorized by the DARDAR-MASK during Austral winter (solid lines) and summer (dashed lines). (left) Relative frequencies of the cloud top phase classes for the single layer of the highest cloud tops (60 m). (right) Relative frequencies of the cloud top phase classes for cloud tops exaggerated to include the top 10 layers (600 m). W: Wintertime; S: Summertime.

vertical resolution etc.), the results, with minimized discrepancies through spatial and temporal averaging, permit a better insight of the climatological signal.

3. Cloud Top Thermodynamic Phase Climatology

[17] The low-elevation clouds over the SO are a major component to the albedo of $\sim 15\%$ of the Earth's surface. The MSM11 cloud top thermodynamic phase (CTP) climatology, produced strictly with MODIS observations, was limited to observations from the 8.5 and 11 μm radiometer channels. The algorithm employed to derive the CTP observations [Platnick *et al.*, 2003] is conservative in that it can readily return an uncertain classification, particularly when the cloud top temperature (CTT) is between -10 and -20°C [Nasiri and Kahn, 2008]. In MSM11, over half of all CTP observations were classified as UN in this temperature range. Being made from a passive sensing instrument, the MODIS climatology is further limited due to screening from overhead cirrus. MSM11 found that a seasonal cycle in the overhead cirrus imprinted a seasonal cycle in low-elevation clouds. The active remote sensing observations of the CPR and CALIOP have the potential to overcome such a limitation.

[18] Approximately, 2500 DARDAR-MASK and CALIPSO images were processed for the four years 2006–2009 with the Austral winter (summer) being defined as June, July, and August (December, January, and February). All granules that reside over the domain of 100 – 160°E and 40 – 65°S were selected, with each individual footprint assigned to a 1° latitude band. East-West variations were not considered

in this study due to the relative uniformity compared with North-South gradients.

[19] Over these 25 latitude bands, the statistics of each CTP categorized by the DARDAR-MASK simplified categorization during both winter and summer are derived. Bins assigned by a phase of liquid warm (LW), supercooled liquid water (SLW), ice phase (ICE), mixed-phase (MIXED), rain (RAIN) or uncertain (UN) were classified as cloudy bins. In principle, UN suggests a likelihood of either liquid water (if temperature lower than 0°C) or aerosol (if temperature greater than 0°C), but has a small possibility to be ice. The relative frequency (RF), defined by the occurrence of an individual class relative to all categories except insects, stratospheric features, ground and clear, has been adapted for the analysis. Aerosol has also been omitted in the CTP statistics. The absolute frequency (AF), with all other classes (i.e., aerosol, insects, stratospheric features, ground and clear) included, is further employed to examine the vertical structures of cloud phase profiles. Cloud top is defined as the highest elevation of 'cloudy' layer in a given column from surface to 30 km. As discussed in Mace *et al.* [2009], active remote sensing of these clouds reveals the frequent presence of multiple layers.

[20] Figure 3 (left) shows the RF of the CTP classes of ICE, MIXED, LW, SLW, RAIN and UN categorized by the DARDAR-MASK during winter (solid lines) and summer (dashed lines) for the single layer (60 m) of the highest cloud top (the highest pixel identified as cloud). The CTP climatology is reconstructed in Figure 3 (right) when the definition of cloud top is exaggerated to include the top 10 layers

(600 m) of vertical pixels. Focusing on Figure 3 (left) first, it is found that ICE is the dominant class with an RF between 0.6 and 0.7 (0.5 and 0.6) during winter (summer). Overall, there is considerably more ICE present than in MSM11, which is to be expected: CALIOP is far more capable of picking up thin layers of overlying cirrus. The seasonal cycle in the RF of ICE is consistent with MSM11, with ICE being more commonly observed over the winter. In winter the RF of ICE is roughly independent of latitude south of 50°S but drops off at the lower latitudes. In summer, the RF of ICE peaks at around 51°S, consistent with the mean location of the SO storm track [Simmonds and Keay, 2000]. The next most common class is SLW, which peaks at 0.25 (0.40) during the winter (summer) at the higher latitudes. The meridional dependence is much stronger in summer than in winter. LW is virtually non-existent south of 55°S but increases strongly at the lower latitudes, particularly during the summer. Not surprisingly, LW decreases with latitude and simply reflects the roughly 10°C decrease in sea surface temperature from north to south across the domain. The RF of MIXED is relatively steady between 0.05 and 0.10 over all latitudes during both summer and winter. Compared to MSM11, this absence of UN with the DARDAR-MASK is notable, and it is due to the fact that the lidar signal cannot be attenuated before the cloud tops of the first layer encountered; MSM11 had an RF of ~ 0.20 (0.25) for UN during winter (summer).

[21] The definition of cloud top may, itself, be ambiguous, as the radiances emitted by the cloud can come from range of depths depending on the optical thickness of the upper levels of the cloud. The sensitivity of the DARDAR-MASK CTP climatology to the definition of the cloud top is explored (Figure 3, right) for a cloud top exaggerated to include the top 10 layers (600 m). The purpose of doing this is to examine the transition of the cloud phase population with respect to cloud top depth. Note that cloud top depths of 10 layers (600 m) and 15 layers (900 m) have also been examined (not shown) but offer only marginal differences and little new insight. Comparing the 600 m thickness with the original 60 m thickness (Figure 3, left), one observes an increase in the RF of ICE at the expense of LW and SLW. As shown in Figure 1 42–44°S, it is not uncommon for the DARDAR-MASK to place a layer of SLW over ICE across the SO. While this may be real [Rauber and Tokay, 1991; Shupe et al., 2004; Wang et al., 2004; Turner, 2005; Verlinde et al., 2007; Edward et al., 2010], this may also be a consequence of the DARDAR-MASK algorithm, when the lidar signal becomes extinct under cloud top and the phase is determined by the radar signal and the ECMWF temperature alone. It should be noted that there are limited in situ observations of thick layers of SLW over the SO [e.g., Morrison et al., 2009]. Also, different from Figure 3 (left), classes of RAIN and UN become more evident.

[22] It is of particular interest to construct a direct comparison of the CTP climatology of the DARDAR-MASK with that of MODIS as calculated in MSM11. In Figure 4, the CTP as seen by DARDAR-MASK and MODIS (MSM11) is sorted by CTT and compared for per individual temperature category. It should be noted that instead of temperature, the wet bulb temperature has been used for the classification in DARDAR-MASK. Given the fact that nearly all the clouds observed by MODIS in MSM11 resided in the temperature

range between 20 to -65°C , the calculation of the CTP for the DARDAR-MASK has only considered clouds within this range. Specifically, clouds with temperature below -65°C , typically high-altitude cirrus, have been excluded.

[23] In comparing the DARDAR-MASK against the MSM11 climatology, the most immediate difference is the substantial glaciated clouds detected at temperatures below -50°C by the DARDAR-MASK. This is primarily attributed to the enhanced detection of overlying cirrus by CALIOP.

[24] Taking the CTT as a proxy of cloud top height, it is notable that the majority of cloud tops detected by MODIS are much lower in height compared against those observed by the DARDAR-MASK. This is particularly evident when comparing the population of cloud tops with temperatures above 0°C . Despite the complication induced by multilayer interference, these low-altitude warm clouds, typically being optically thin, could have potentially been missed by both the CPR and CALIOP observations, as suggested by Chan and Comiso [2011].

[25] At temperatures warmer than -20°C , the shape of these distributions is roughly similar, but the composition is not. At these warmer temperatures the DARDAR-MASK observes virtually no UN, but considerable ICE, while MSM11 recorded UN but virtually no ICE. One might initially assume that this is simply evidence of a more decisive algorithm for the DARDAR-MASK: what was originally classified as UN for MODIS is classified as ICE. This assumption fails when looking at the CTT between 0°C and -10°C . During the winter between 40 and 50°S the DARDAR-MASK has an RF ~ 0.09 for ICE, which could not arise by reclassifying the UN in the MSM11 climatology. This inconsistency is exacerbated when including the MIXED class. The DARDAR-MASK detects considerable MIXED cloud tops in this temperature range. While it may be natural to give more weight to the more sophisticated climatology of the DARDAR-MASK, this remains to be verified in such a unique environment as that over the Southern Ocean. These results, therefore, should be treated with caution as they have not been verified with in situ observations. As suggested in the examples, the DARDAR-MASK commonly records ICE or MIXED at cloud tops where CALIPSO records only liquid water.

[26] It is further of interest to consider the seasonal differences in the CTP versus CTT graphs (Figure 4). During winter, when there is more overlying cirrus, the DARDAR-MASK observes both SLW (primarily) and some ICE between 0 and -20°C . During the summer, when there is less overhead cirrus, SLW is more common, particularly at the higher latitudes. SLW also dominated the CTP for this temperature range in the MSM11 climatology. This seasonal shift in CTP may indeed, be real. It may also be a consequence of the seasonal shift in the overlying cirrus as this cirrus can readily affect the ability of the lidar to observe the clouds in the temperature range of 0 to -20°C . Very thick overlying cirrus can even fully attenuate the lidar signal, meaning that the low level clouds are being detected by the radar alone. Such a scenario will almost certainly lead to the CTP including some ICE.

[27] Another potential bias in the CALIPSO observations is that the overlying cirrus may affect the CTP classification of the low-elevation clouds. This hypothesis can be tested by

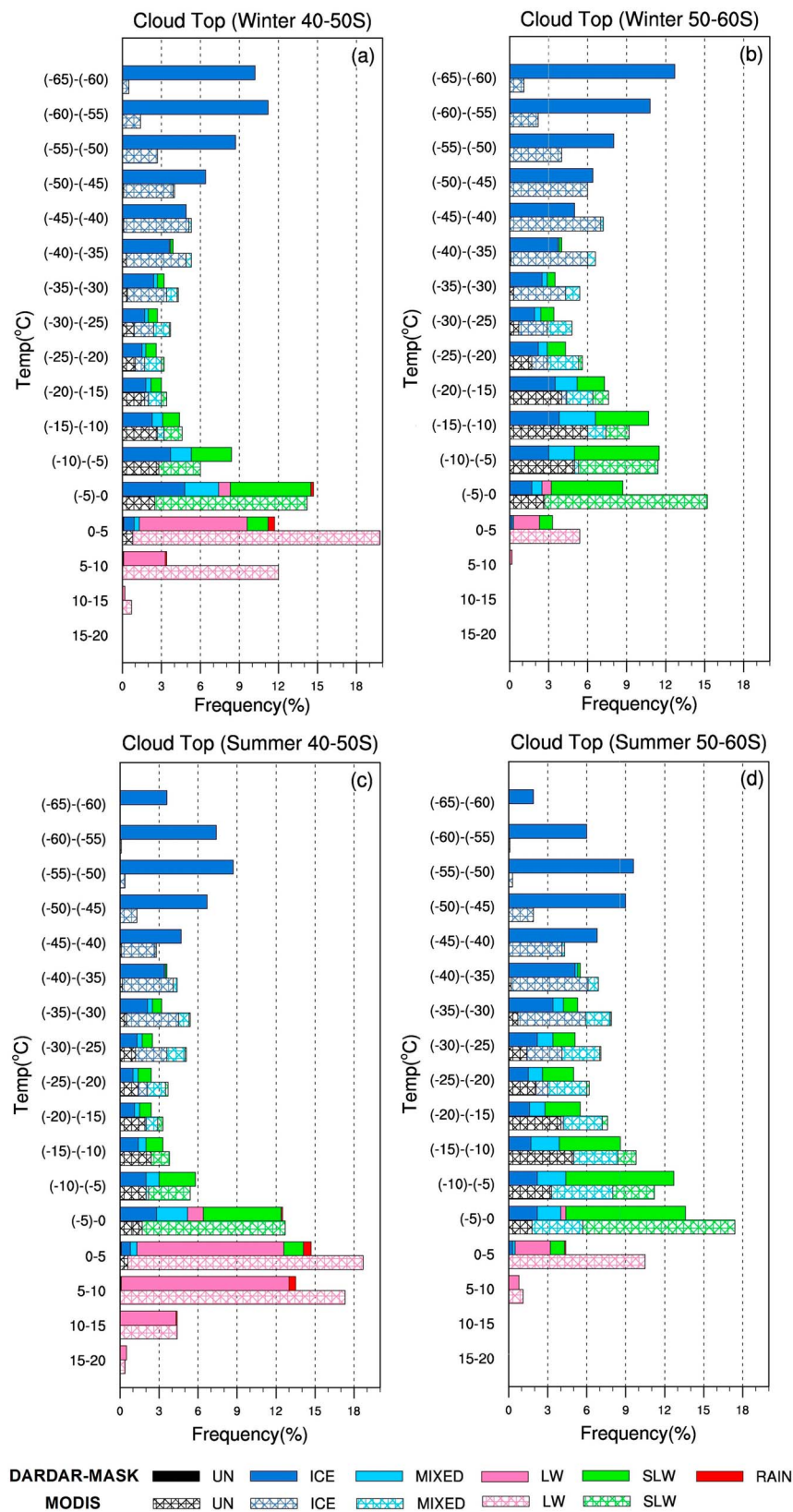


Figure 4. Histograms showing the relative frequencies (RFs) of cloud top temperatures decomposed into their constituent phases (ICE, MIXED, LW, SLW, RAIN and UN): (a) winter 40–50°S, (b) winter 50–60°S, (c) summer 40–50°S, and (d) summer 50–60°S. For MODIS, the class occurrence is relative to the total time. For DARDAR-MASK, the class occurrence is relative to the time that the observed cloud resides in the temperature range of 20 to –65°C.

Table 1. Fractional Cloud Cover Derived by CALIPSO During Winter and Summer for All Clouds, Clouds Observed Above 5 km Only and Clouds Existing Below 5 km^a

	Winter			Summer		
	Coverage	Liquid	ICE	Coverage	Liquid	ICE
Cloudy	88.3%			87.0%		
Clouds >5 km only	14.2%			12.6%		
With clouds <5 km	74.1%			74.4%		
No overhead	38.2%	85.5%	14.5%	47.5%	91.2%	8.8%
With overhead	25.1%	76.0%	23.2%	19.4%	77.4%	22.6%
Solid clouds across 5 km	10.8%			7.5%		

^aRelative frequencies (RFs) of ice and liquid phase cloud tops are shown by segregating the low-elevation clouds with respect to the presence of overlying cirrus.

segregating the low-elevation clouds with respect to the presence of overlying cirrus. In Table 1, the CALIPSO observations over the domain of interest are analyzed. Different from the DARDAR-MASK, the phase partition in CALIPSO VFM applies both the lidar backscatter, polarization and their layer continuity to analyze the sphericity of the hydrometeors. It is noted that CALIPSO observes a very weak seasonal variation in the total fractional cloud cover (defined by cloud frequency of occurrence as seen from a passive remote sensing satellite): 88.3% during wintertime and 87.0% during summertime. This may be further broken down by the altitude of the cloud layer. 14.2% (12.6%) of the time CALIPSO records cloud but only at elevations above of 5 km during winter (summer). This includes not only simple cirrus clouds overlying clear air, but also thick cirrus clouds or frontal clouds that have penetrated above

5 km (Example 1: around 43°S) and completely attenuate the lidar signal below (including passing through) 5 km. This is similar to the 10 to 12% frontal cloud structure found by Mace [2010].

[28] The remaining observations, 74.1% (74.4%) for winter (summer), have some cloud present at an elevation of 5 km or less, which can be broken down yet further. In winter (summer) CALIPSO recorded low cloud without any overlying cloud (above 5 km) 38.2% (47.5%) of the time (e.g., Example 2: 45–50°S), low cloud with an overlying layer of cloud 25.1% (19.4%) (e.g., Example 1: 46–53°S), or low cloud with cloud passing through the 5 km elevation 14.2% (12.6%) (e.g., Example 1: 61–63°S). Focusing on the phase of the low cloud, a sensitivity is observed to the presence of overlying cloud. When no overhead cloud is present, CALIPSO is more likely to record liquid water (supercooled and warm) than ICE. A potential bias might exist in that both the lidar backscatter and the infrared emission are most sensitive to the top 2 to 3 optical depths of the cloud; hence the phase of the clouds with overhead coverage could be misidentified as either water or ice, depending on what dominates the signal of the top optical depths. Since high-level cirrus clouds are typically glaciated, the fraction of supercooled liquid water present may be underestimated [Hu et al., 2010]. However, it is unclear whether this feature is a contamination or a real atmospheric state modified by the incoming and outgoing radiation through the overlying cirrus deck. Given that there is a strong seasonal cycle in the amount of high-altitude cloud cover, there is a potential that an artificial seasonal cycle is imprinted on the phase of the low-elevation clouds.

[29] Similar to the CALIPSO observations of Table 1, the DARDAR-MASK observations of CTP can be screened to look at low-elevation clouds (highest cloud top below 5 km

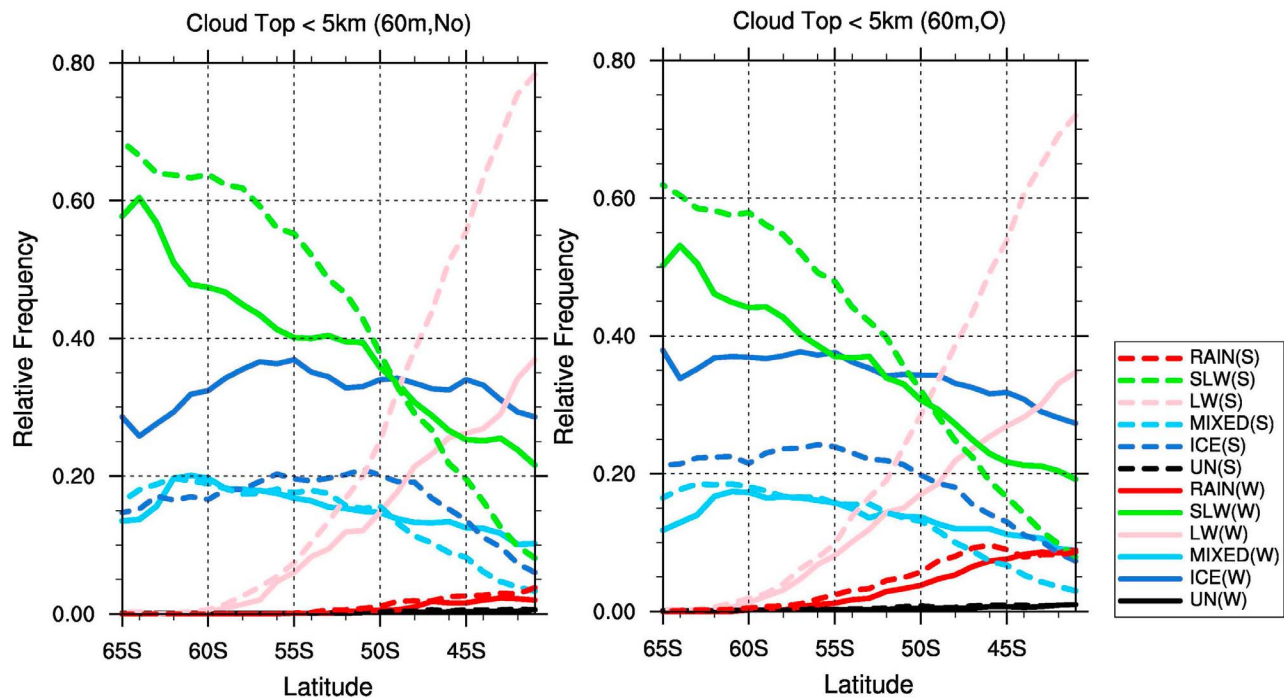


Figure 5. Same as Figure 3 left for the single layer of the highest cloud tops below 5 km. (left) Cloud tops without overhead cloud being present (No). (right) Cloud tops with overhead cloud being present (O).

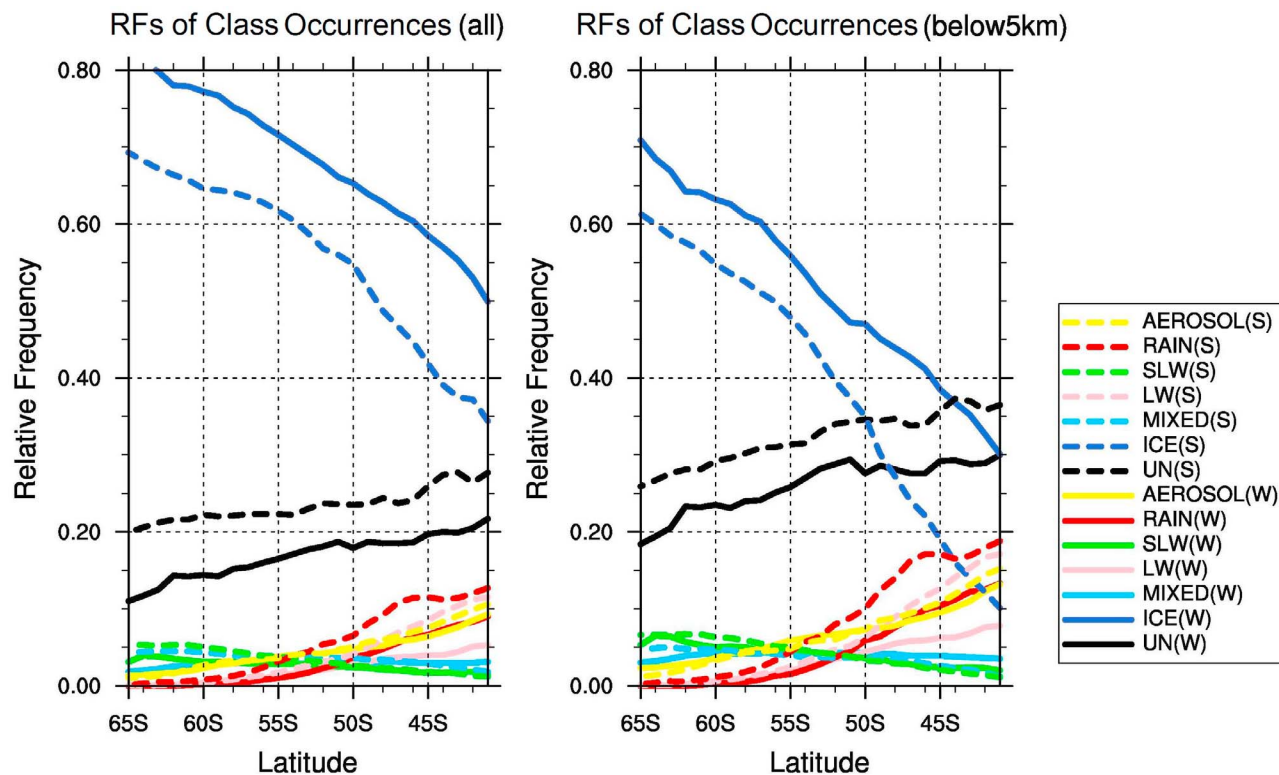


Figure 6. Relative frequencies (RFs) of the classes of ice (ICE), mixed-phase (MIXED), liquid warm (LW), supercooled liquid water (SLW), rain (RAIN), aerosol (AEROSOL) and uncertainty (UN) categorized by DARDAR-MASK as a function of latitude. (left) Relative frequencies of class occurrences through the whole atmosphere observed. (right) Relative frequencies of class occurrences within the lowest 5 km. W: Wintertime; S: Summertime.

altitude) without (Figure 5, left) and with (Figure 5, right) overhead cloud being present. It should be noted that this is not identical to the filtering used for CALIPSO-only observations, as the CPR signals are not readily attenuated by thick cirrus. The most immediate difference in comparing the CTP of low-elevation clouds with the overall CTP (Figure 3) is the reduction in the RF of ICE. The RF of ICE drops to between 20 and 40% and the RFs of the other classes increase accordingly, most noticeably for SLW. When isolating the effect of the presence of overlying cirrus on the low-elevation clouds, a further change in the RF of ICE is evident. The RF of ICE in the low-elevation clouds is greater when high-altitude clouds are present, and this more commonly occurs during winter.

[30] A broader comparison of the CTP between MODIS, CALIPSO and the DARDAR-MASK may be undertaken. During the winter (summer) months, CALIPSO records ICE somewhere between 14.5% (8.8%) and 23.2% (22.6%) of the time for these low elevation clouds depending on whether they are screened by high-elevation clouds. In MSM11, MODIS recorded virtually no ice for these low-elevation clouds, but considerable UN. The integrated DARDAR-MASK climatology (not shown) finds that roughly 35% (20%) of such cloud tops should consist of ICE in winter (summer). In comparison to either CALIPSO or MODIS, the DARDAR-MASK more frequently records ICE as the CTP for clouds between 0 and -20°C . In addition to this, MIXED class is more commonly recorded by the DARDAR-MASK

as the CTP for low-elevation clouds over the SO, compared to MODIS.

4. Class Occurrences and Vertical Distributions

[31] The key benefit of active remote sensing is the ability to move beyond cloud top or column integrated observations to examine the cloud phase properties throughout the depth of the atmosphere. In Figure 6 (left), the RFs of the classes assigned by the DARDAR-MASK are presented with the minor contributions of insects, stratospheric features and ground removed. ICE is the dominant phase through the region in both winter and, to a lesser extent, summer. Much of this ICE resides at colder temperatures ($<-40^{\circ}\text{C}$) as illustrated in Figure 4. The next most dominant class is, UN, with a peak of ~ 0.2 (0.3) at the low latitudes decreasing to ~ 0.1 (0.2) at the high latitudes for winter (summer). This may be somewhat surprising given the RF of UN was less than 0.01 at cloud top. The examples illustrate that the DARDAR-MASK may readily produce UN below cloud top. UN arises not only from thick frontal clouds (e.g., Example 1: $42-44^{\circ}\text{S}$) but also for lower boundary layer clouds (e.g., Example 1: $50-56^{\circ}\text{S}$). At the lower latitudes the RF of AEROSOL, RAIN, LW can approach 0.1 with a slightly greater RF during summer when there is less ICE. The RF of LW actually displays a strong seasonal cycle ranging between ~ 0.05 in winter (at 40°S) to ~ 0.11 during summer at these lower latitudes.

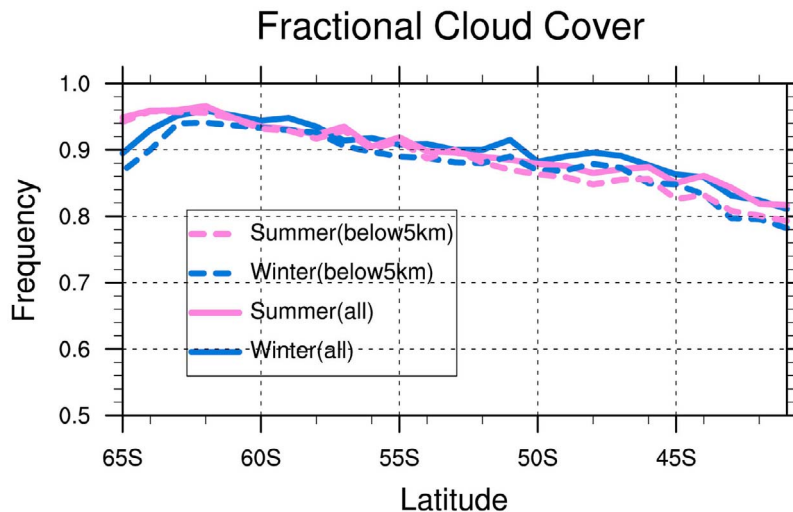


Figure 7. Fractional cloud cover over 40–65°S, 100–160°E during both winter and summer for all clouds and low-elevation clouds below 5 km. Fractional cloud cover is defined by the cloud frequency of occurrence as seen from a passive remote sensing satellite.

[32] The RFs of class occurrences can be limited to retrievals through the lowest 5 km altitude over the SO (Figure 6, right). Not surprisingly, when high-altitude cirrus clouds are removed from the system, the RF of ICE decreases and the RFs of the other classes increase. This is most evident at low latitudes during the summer where the RF of ICE drops to ~ 0.1 .

[33] Returning to the full data set, the sum of the non-clear classes gives a measure of the fractional cloud cover (defined by cloud frequency of occurrence as seen from a passive remote sensing satellite) in Figure 7, which ranges from 0.96 at 60°S to 0.81 at 40°S. Except between 60 and 65°S, there is remarkably little seasonal variation given the significant seasonal cycle of sea surface temperature. The fractional cloud cover for the low-elevations clouds (clouds below 5 km) ranges between 0.8 and 0.95. However, this maybe an underestimate compared against MODIS climatology considering again the low-altitude warm clouds being missed by both CPR and CALIOP as discussed by *Chan and Comiso* [2011].

[34] Finally the absolute frequencies (AF) of class occurrences can be examined as a function of depth (Figure 8) across the full domain (40 to 65°S). Once again it is evident that the cloud fraction experiences only a weak seasonal cycle. Clear sky is recorded 65% (68%) of the time at a height of 3 km in winter (summer) and 20% (17%) of the time at a height of 700 m. The steepest gradient on cloud frequency of occurrence is between 700 and 1700 m with clouds below a depth of 700 m dominating over the SO. Again, it is most unfortunate that the CPR cannot reliably be interpreted at low level. For many classes the profile can be broken up into three rough altitude bands: below 700 m where no CPR is available, from ~ 700 to ~ 1000 m when the first layer of CPR becomes available, and above 1000 m.

[35] Focusing on the individual classes, ICE is observed to undergo a substantial seasonal cycle with higher AF observed at all altitudes during winter. LW undergoes a weaker seasonal cycle, although it is observed at much greater heights during summer. SLW is observed throughout the full range of the

domain with the peak AF between 700 and 1000 m. The MIXED class does not exist below 700 m when only the CALIOP signal is available. MIXED peaks at around 1500 m (1800 m) in winter (summer). Like SLW it is found up through the lower free troposphere. The MIXED class is a direct consequence of the DARDAR-MASK algorithm, where CALIOP returns liquid water and the CPR returns a signal in the temperature range of 0 to -20°C . Taken collectively LW + SLW + MIXED displays a consistent seasonal cycle. During winter, when the temperatures are colder, this group is more prevalent at lower elevations; during the summer it shifts to slightly higher elevations. The RAIN class is most prevalent through this lowest 700 m with the peak AF reaching 0.08 (0.11) in winter (summer). In summer RAIN is evident up to a height of 3000 m while in winter it essentially terminates around 2000 m. This result is expected as the altitude of precipitating layer is directly deduced from temperature.

[36] The AEROSOL class is perhaps the most difficult to appreciate without in situ observations. It is interesting to observe AEROSOL up to heights of 2000 m undergoing virtually no seasonal cycle (note that the AEROSOL in DARDAR-MASK is rigorously adapted from the CALIPSO VFM). As discussed in the introduction, the importance of aerosol in the formation of cloud and precipitation has been highlighted in independent studies and climate feedback hypotheses. *Woodcock* [1953] examined the vertical gradients in sea salt aerosol and found that increases in the amount of airborne salt near cloud base in marine air are related to increases in wind force at the sea surface. The CLAW hypothesis has been the subject of active research for over 20 years. More recently, *Korhonen et al.* [2010] noted that the albedo of the low-altitude clouds would respond directly to changes in the amount of sea spray, resulting from the increase of surface wind caused by the strengthening of westerly jet in the Southern Hemisphere over the past four decades. Thus one hypothesis for the AEROSOL being recorded by the DARDAR-MASK is that they are likely to be evidence of sea spray. The CALIPSO aerosol product provides the classification of the aerosol types [*Omar et al.*, 2009].

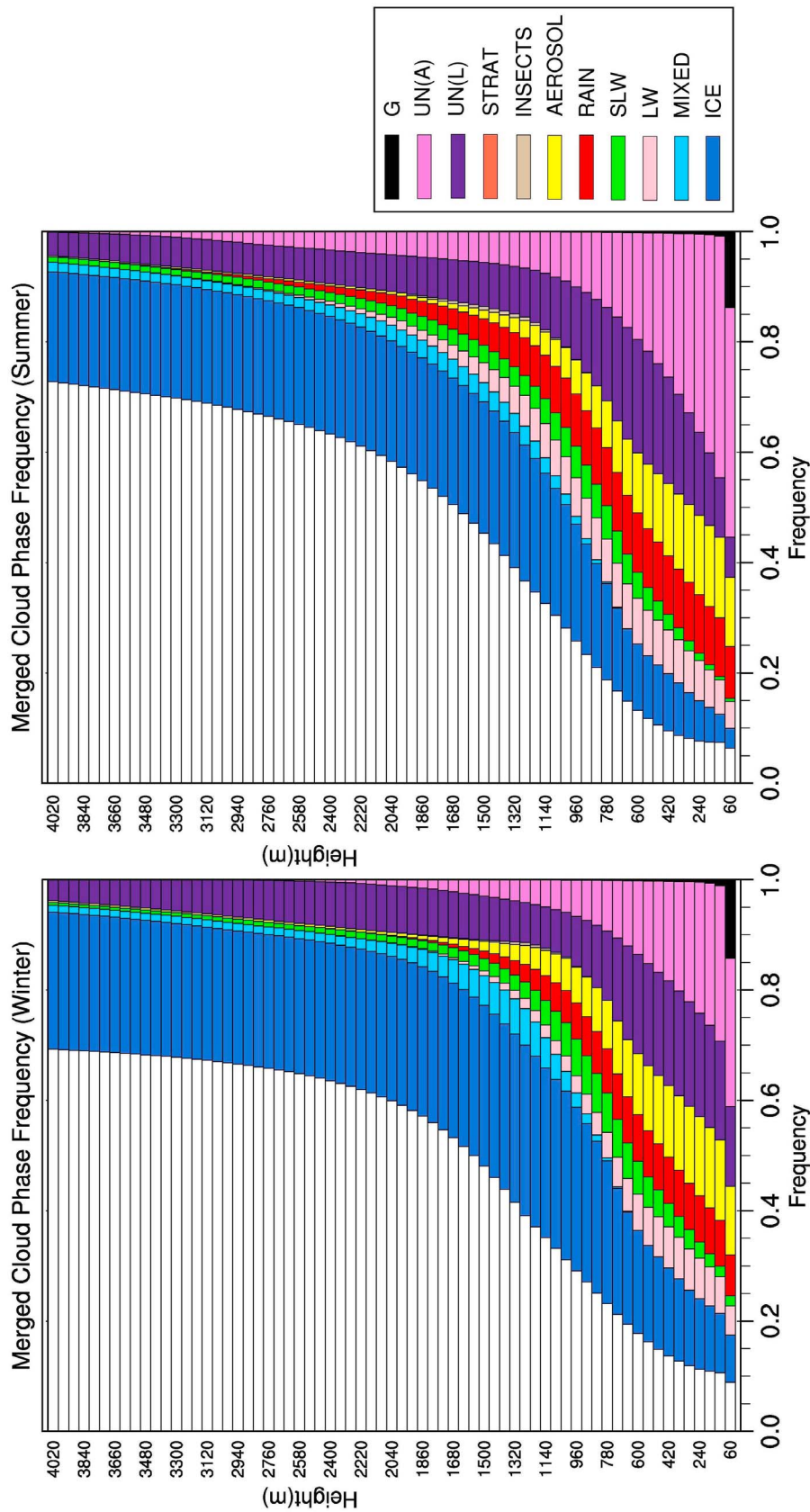


Figure 8. Absolute frequencies (AF) of the classes categorized by DARDAR-MASK as a function of depth in (left) winter and (right) summer. UN(A): UN that may be aerosol; UN(L): UN that may be liquid water; STRAT: stratospheric features.

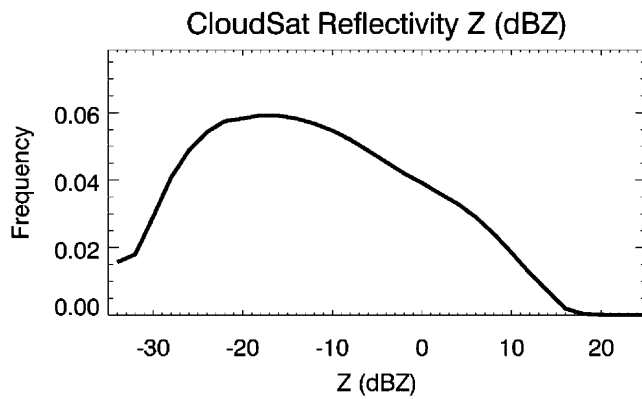


Figure 9. The probability distribution function of CPR reflectivities derived from all CloudSat observations between 30 to 60°S in year 2007.

[37] The UN class is the dominant class across the lowest 700 m with an AF of ~ 0.4 (~ 0.5) during winter (summer). This again reflects the challenge in observing the clouds across the SO and trying to improve the energy and water budgets. The UN class most clearly displays the three height bands of 0–700 m, 700–1000 m and above arising from the physical limitations of the CPR and complete extinction of the lidar signal below optically thick layers (see example of Figure 2 around 60°S). At heights above 2000 m, the UN has an AF of ~ 0.10 in both winter and summer and may be interpreted as a measure of the frequency of heavy frontal clouds that attenuate both the CALIOP and the CPR. Below 700 m it is more difficult to interpret as the lidar signal may attenuate quickly and there is no CPR signal available. While it is entire possible that some of the UN could be clear sky lying beneath stratocumulus-like decks that are thick enough to block out CALIOP, the underestimate of low-elevation clouds due to the physical limitation of CloudSat could be the reason.

[38] In Figure 9, the probability distribution function of CPR reflectivities shows that with the current CPR sensitivity of -31 dBZ [Protat *et al.*, 2009], a relatively large frequency of cloud occurrence is still detected. This observed cutoff at the lower limit clearly however suggests that CloudSat is missing a significant portion of clouds with reflectivities below -31 dBZ. This range of clouds is more likely to be within the boundary layer.

5. Conclusions

[39] The DARDAR-MASK has been used to examine the structure of clouds over the Southern Ocean (SO) for the four-year period of 2006–2009 during both winter (June–August) and summer (December–February). Low-elevation clouds are dominant across this region year-round with very little seasonal cycle being evident. This would suggest that solar radiation is not a first order effect in their formation and maintenance. The fractional cloud cover for clouds at heights beneath 5 km ranges from 0.80 at the low latitudes (40°S) to 0.95 at the high latitudes (60°S).

[40] The bulk of this cloud mass is found at heights less than 1 km, which is problematic for the observations due to

the physical limitation of the CPR and the common extinction of CALIOP. In summer (winter) the AF of UN was ~ 0.5 (0.4) in this layer. The relatively coarse vertical resolution of the CPR (500 m) means that the layer between ~ 700 and 1000 m, where the CPR is first reliably available, commonly displays the strongest gradients in class. Above this band the AFs of the classes are weakly dependent on height.

[41] The CPR is further limited across the SO as the vast majority of these low-altitude clouds exist in the temperature range of 0 to -20°C . Any algorithm interpreting the CPR reflectivity must assign thermodynamics phase in this range. Given the strong temperature gradient in the sea surface temperature over the SO, any cloud phase assignment will likely display strong meridional gradients.

[42] Focusing on the cloud top phase (CTP), a comparison has been made between the CALIPSO cloud phase mask, the DARDAR-MASK and the MODIS only climatology of MSM11. Similar to the MODIS climatology, CALIPSO suggests that liquid water dominates the CTP of low-elevation clouds across the SO with a RF of ~ 0.82 (0.87) during winter (summer). This is a more definitive calculation than MSM11, which suffered from a large frequency (~ 0.30) of UN. However, challenges remain when considering the geometrically thin clouds near the surface that are apparently present in MODIS but could possibly be missed by both the CPR and CALIOP, as discovered by Chan and Comiso [2011]. Given the exceptional prevalence of low-altitude cloud over the SO, the bias introduced by the nature of the instruments might have a remarkable impact on accurately characterizing the radiative signature. It was also observed that the CALIPSO climatology is sensitive to the presence of overlying cirrus. If the lidar can see through the overlying cirrus, it is more likely to record ICE as the CTP of the low-elevation clouds. Given that there is more cirrus evident during winter, this screening effect can produce an artificial seasonal cycle on the CTP of the low-elevation clouds.

[43] The DARDAR-MASK, by comparison, finds more ICE and MIXED at cloud top than either CALIPSO or MODIS for these low-elevation cloud types. This is likely to be a consequence of the limitations of the CPR filtering through the DARDAR-MASK algorithm at a temperature below 0°C . It is also possible that a screening effect of overlying cirrus occurs in CALIOP and flows through to the DARDAR-MASK CTP climatology.

[44] One of the remarkable features has been the non-negligible observation of aerosol over the Southern Ocean. The AF can surpass 0.15 through the lowest 1000 m with no seasonal cycle. It is likely that the aerosol recorded by the DARDAR-MASK is dominated by sea spray, as the Southern Ocean is a region of intense surface wind speed [Young *et al.*, 2011]. It was of further interest to find that aerosol was observed up to heights of 2000 m over the SO.

[45] The aim of this research has been to derive and compare satellite cloud climatologies over the SO from various platforms. It has highlighted the ambiguity in spaceborne sensed cloud properties over the SO and the challenge that remains in better defining the energy and water budget, as highlighted by Trenberth and Fasullo [2010]. A dedicated field campaign with the application of the ground-based radar-lidar-microwave radiometer and aircraft in situ observations (such as the ARM Mobile

Facility or Australian National Marine Facility observation) is necessary for this unique environment.

Notation

AEROSOL	Aerosol
AF	Absolute Frequency
AMSR-E	Advanced Microwave Scanning Radiometer
CALIPSO	Cloud-Aerosol Lidar and Infrared Pathfinder Satellite Observations
CALIOP	Cloud-Aerosol Lidar with Orthogonal Polarization
CCN	Cloud Condensation Nuclei
CERES	Clouds and the Earth's Radiant Energy System
CLAW	Charlson, Lovelock, Andreae and Warren
CPR	Cloud Profiling Radar
CTP	Cloud top Thermodynamic Phase
CTT	Cloud top Temperature
DARDAR-MASK	raDAR/lidar-MASK
ECMWF	European Centre for Medium-Range Weather Forecasts
ICE	Ice
LIQUID	Liquid
LW	Liquid Warm
MIXED	Mixed-phase
MODIS	Moderate Resolution Imaging Spectroradiometer
MSM11	Morrison et al. [2011]
RAIN	Rain
RF	Relative Frequency
SLW	Supercooled Liquid Water
SO	Southern Ocean
UN	Uncertain
VFM	Vertical Feature Mask

[46] **Acknowledgments.** The authors thank MODIS, CloudSat and CALIPSO teams for the assistance donating data. Thanks to the ICARE Data and Services Center (<http://www.icare-lille1.fr>) for providing access to the space-borne data used in this study. We have also benefited from discussions with Yongxiang Hu and Stuart Young.

References

- Anselmo, T., et al. (2006), Cloud Aerosol Lidar Infrared Pathfinder Satellite Observations (CALIPSO) data management system and data products catalog, release 2.3, *Doc. PCSCI-503*, NASA Langley Res. Cent., Hampton, Va.
- Ayers, G. P., and J. M. Cainey (2007), The CLAW hypothesis: A review of the major developments, *Environ. Chem.*, *4*(6), 366–374, doi:10.1071/EN07080.
- Boers, R., J. B. Jensen, and P. B. Krummel (1998), Microphysical and short-wave radiative structure of marine stratocumulus clouds over the Southern Ocean: Summer results and seasonal differences, *Q. J. R. Meteorol. Soc.*, *124*, 151–168, doi:10.1002/qj.49712454507.
- Chan, M. A., and J. C. Comiso (2011), Cloud features detected by MODIS but not by CloudSat and CALIOP, *Geophys. Res. Lett.*, *38*, L24813, doi:10.1029/2011GL050063.
- Charlson, R. J., et al. (1987), Oceanic phytoplankton, atmospheric sulphur, cloud albedo and climate, *Nature*, *326*(6114), 655–661, doi:10.1038/326655a0.

- Delanoë, J., and R. J. Hogan (2008), A variational scheme for retrieving ice cloud properties from combined radar, lidar, and infrared radiometer, *J. Geophys. Res.*, *113*, D07204, doi:10.1029/2007JD009000.
- Delanoë, J., and R. J. Hogan (2010), Combined CloudSat-CALIPSO-MODIS retrievals of the properties of ice clouds, *J. Geophys. Res.*, *115*, D00H29, doi:10.1029/2009JD012346.
- Edward, P. L., P. Kollias, and M. D. Shupe (2010), Detection of supercooled liquid in mixed-phase clouds using radar Doppler spectra, *J. Geophys. Res.*, *115*, D19201, doi:10.1029/2009JD012884.
- Gras, J. L. (1995), CN, CCN and particle size in Southern Ocean air at Cape Grim, *Atmos. Res.*, *35*, 233–251, doi:10.1016/0169-8095(94)00021-5.
- Hande, L. B., S. T. Siems, M. J. Manton, and D. Belusic (2012), Observations of wind shear over the Southern Ocean, *J. Geophys. Res.*, *117*, D12206, doi:10.1029/2012JD017488.
- Hu, Y., et al. (2009), CALIPSO/CALIOP cloud phase discrimination algorithm, *J. Atmos. Oceanic Technol.*, *26*, 2293–2309, doi:10.1175/2009JTECHA1280.1.
- Hu, Y., S. Rodier, K. Xu, W. Sun, J. Huang, B. Lin, P. Zhai, and D. Josset (2010), Occurrence, liquid water content, and fraction of supercooled water clouds from combined CALIOP/IR/MODIS measurements, *J. Geophys. Res.*, *115*, D00H34, doi:10.1029/2009JD012384.
- Huang, Y., et al. (2012), The structure of low-altitude clouds over the Southern Ocean as seen by CloudSat, *J. Clim.*, *25*, 2535–2546, doi:10.1175/JCLI-D-11-00131.1.
- Im, E., et al. (2006), Cloud profiling radar for CloudSat mission, *IEEE Trans. Aerosp. Electron. Syst.*, *20*, 15–18, doi:10.1109/MAES.2005.1581095.
- Korhonen, H., K. S. Carslaw, P. M. Forster, S. Mikkonen, N. D. Gordon, and H. Kokkola (2010), Aerosol climate feedback due to decadal increases in Southern Hemisphere wind speeds, *Geophys. Res. Lett.*, *37*, L02805, doi:10.1029/2009GL041320.
- Mace, G. G. (2010), Cloud properties and radiative forcing over the maritime storm tracks of the Southern Ocean and North Atlantic derived from A-Train, *J. Geophys. Res.*, *115*, D10201, doi:10.1029/2009JD012517.
- Mace, G. G., Q. Zhang, M. Vaughan, R. Marchand, G. Stephens, C. Trepte, and D. Winker (2009), A description of hydrometeor layer occurrence statistics derived from the first year of merged CloudSat and CALIPSO data, *J. Geophys. Res.*, *114*, D00A26, doi:10.1029/2007JD009755.
- Morrison, A. E., et al. (2009), On the analysis of a cloud seeding data set over Tasmania, *J. Appl. Meteorol. Clim.*, *48*, 1267–1280, doi:10.1175/2008JAMC2068.1.
- Morrison, A. E., S. T. Siems, and M. J. Manton (2011), A cloud-top phase climatology of Southern Ocean clouds, *J. Clim.*, *24*, 2405–2418, doi:10.1175/2010JCLI3842.1.
- Mossop, S. C., A. Ono, and E. R. Wishart (1970), Ice particles in maritime near Tasmania, *Q. J. R. Meteorol. Soc.*, *25*, 487–508.
- Nasiri, S. L., and B. H. Kahn (2008), Limitations of bi-spectral infrared cloud phase determination and potential for improvement, *J. Appl. Meteorol. Climatol.*, *47*(11), 2895–2910, doi:10.1175/2008JAMC1879.1.
- Omar, A. H., et al. (2009), The CALIPSO automated aerosol classification and lidar ratio selection algorithm, *J. Atmos. Oceanic Technol.*, *26*, 1994–2014, doi:10.1175/2009JTECHA1231.1.
- Platnick, S., et al. (2003), The MODIS cloud products: Algorithms and examples from Terra, *IEEE Trans. Geosci. Remote Sens.*, *41*(2), 459–473, doi:10.1109/TGRS.2002.808301.
- Protat, A., et al. (2009), Assessment of Cloudsat reflectivity measurements and ice cloud properties using ground-based and airborne cloud radar observations, *J. Atmos. Oceanic Technol.*, *26*(9), 1717–1741, doi:10.1175/2009JTECHA1246.1.
- Rauber, R. M., and A. Tokay (1991), An explanation for the existence of supercooled water at the top of cold clouds, *J. Atmos. Sci.*, *48*, 1005–1023, doi:10.1175/1520-0469(1991)048<1005:AEFTEO>2.0.CO;2.
- Ryan, B. F., and W. D. King (1997), A critical review of the Australian experience in cloud seeding, *Bull. Am. Meteorol. Soc.*, *78*, 239–254, doi:10.1175/1520-0477(1997)078<0239:ACROTA>2.0.CO;2.
- Shupe, M. D., et al. (2004), Deriving mixed-phase cloud properties from Doppler radar spectra, *J. Atmos. Oceanic Technol.*, *21*, 660–670, doi:10.1175/1520-0426(2004)021<0660:DMCPFD>2.0.CO;2.
- Simmonds, I., and K. Keay (2000), Mean Southern Hemisphere extratropical cyclone behaviour in the 40-year NCEP-NCAR reanalysis, *J. Clim.*, *13*, 873–885, doi:10.1175/1520-0442(2000)013<0873:MSHECB>2.0.CO;2.
- Stephens, G. L., et al. (2002), The CloudSat mission and the A-Train: A new dimension of space-based observations of clouds and precipitation, *Bull. Am. Meteorol. Soc.*, *83*, 1771–1790, doi:10.1175/BAMS-83-12-1771.
- Tietäväinen, H., and T. Vihma (2008), Atmospheric moisture budget over Antarctica and the Southern Ocean based on the ERA-40 reanalysis, *Int. J. Clim.*, *28*, 1977–1995, doi:10.1002/joc.1684.

- Trenberth, K. E., and J. T. Fasullo (2010), Simulation of present-day and twenty-first-century energy budgets of the Southern Oceans, *J. Clim.*, *23*(2), 440–454, doi:10.1175/2009JCLI3152.1.
- Turner, D. D. (2005), Arctic mixed-phase cloud properties from AERI lidar observations: Algorithm and results from SHEBA, *J. Appl. Meteorol.*, *44*, 427–444, doi:10.1175/JAM2208.1.
- Vallina, S., and R. Simo (2007), Strong relationship between DMS and the solar radiation dose over the global surface ocean, *Science*, *315*, 506–508, doi:10.1126/science.1133680.
- Verlinde, H., et al. (2007), The Mixed-Phase Arctic Cloud Experiment (MPACE), *Bull. Am. Meteorol. Soc.*, *88*, 205–221, doi:10.1175/BAMS-88-2-205.
- Wang, Z., et al. (2004), Studying altocumulus with ice virga using ground-based active and passive remote sensors, *J. Appl. Meteorol.*, *43*, 449–460, doi:10.1175/1520-0450(2004)043<0449:SAWIVU>2.0.CO;2.
- Wentz, F. J., and T. Meissner (2000), AMSR algorithm theoretical basis document, version 2, Remote Sens. Syst., Santa Rosa, Calif.
- Wielicki, B. A., et al. (1998), Clouds and the Earth's Radiant Energy System (CERES): Algorithm overview, *IEEE Trans. Geosci. Remote Sens.*, *36*(4), 1127–1141, doi:10.1109/36.701020.
- Winker, D. M., B. H. Hunt, and M. J. McGill (2007), Initial performance assessment of CALIOP, *Geophys. Res. Lett.*, *34*, L19803, doi:10.1029/2007GL030135.
- Woodcock, A. H. (1953), Salt nuclei in marine air as a function of altitude and wind force, *J. Meteorol.*, *10*, 362–371, doi:10.1175/1520-0469(1953)010<0366:SNIMAA>2.0.CO;2.
- Young, I. R., S. Zieger, and A. V. Babanin (2011), Global trends in wind speed and wave height, *Science*, *332*, 451–455, doi:10.1126/science.1197219.
- Yum, S. S., and J. G. Hudson (2005), Adiabatic predictions and observations of cloud droplet spectral broadness, *Atmos. Res.*, *73*, 203–223, doi:10.1016/j.atmosres.2004.10.006.